*First publ. in: The Journal of Biological Chemistry 275 (2000), 21, pp. 2019-2028*

# Entrance Port for $Na^+$ and $K^+$ Ions on $Na^+,K^+$-ATPase in the Cytoplasmic Loop between Trans-membrane Segments M6 and M7 of the $\alpha$ Subunit

PROXIMITY OF THE CYTOPLASMIC SEGMENT OF THE $\beta$ SUBUNIT*

(Received for publication, July 26, 1999, and in revised form, October 20, 1999)

**Alla Shainskaya‡§, Anne Schneeberger, Hans-Jürgen Apell, and Steven J. D. Karlish‡¶**

*From the ‡Department of Biological Chemistry, Weizmann Institute of Science, 76100 Rehovot, Israel and Department of Biology, University of Konstanz, D-78434 Konstanz, Germany*

**Based on the following observations we propose that the cytoplasmic loop between trans-membrane segments M6 and M7 (L6/7) of the $\alpha$ subunit of $Na^+,K^+$-ATPase acts as an entrance port for $Na^+$ and $K^+$ ions. 1) In defined conditions chymotrypsin specifically cleaves L6/7 in the M5/M6 fragment of 19-kDa membranes, produced by extensive proteolysis of $Na^+,K^+$-ATPase, and in parallel inactivates $Rb^+$ occlusion. 2) Dissociation of the M5/M6 fragment from 19-kDa membranes is prevented either by occluded cations or by competitive antagonists such as $Ca^{2+}$, $Mg^{2+}$, $La^{3+}$, *p*-xylylene bisguanidinium and *m*-xylylene bisguanidinium, or 1-bromo-2,4,6-tris(methylisothiouronium)benzene and 1,3-dibromo-2,4,6-tris (methylisothiouronium)benzene ($Br_2$-TITU$^{3+}$). 3) $Ca^{2+}$ ions raise electrophoretic mobility of the M5/M6 fragment but not that of the other fragments of the $\alpha$ subunit. It appears that negatively charged residues in L6/7 recognize either $Na^+$ or $K^+$ ions or the competitive cation antagonists. $Na^+$ and $K^+$ ions are then occluded within trans-membrane segments and can be transported, whereas the cation antagonists are not occluded and block transport at the entrance port. The cytoplasmic segment of the $\beta$ subunit appears to be close to or contributes to the entrance port, as inferred from the following observations. 1) Specific chymotryptic cleavage of the 16-kDa fragment of the $\beta$ subunit to 15-kDa at 20 °C (Shainskaya, A., and Karlish, S. J. D. (1996) *J. Biol. Chem.* 271, 10309–10316) markedly reduces affinity for $Br_2$-TITU$^{3+}$ and for $Na^+$ ions, detected by $Na^+$ occlusion assays or electrogenic $Na^+$ binding, whereas $Rb^+$ occlusion is unchanged. 2) $Na^+$ ions specifically protect the 16-kDa fragment against this chymotryptic cleavage.**

An understanding of the working of P-type active cation pumps such as $Na^+,K^+$-, $H^+,K^+$-, $H^+$-, and $Ca^{2+}$-ATPase will require knowledge of high resolution molecular structure. The most detailed structures available are those of $Ca^{2+}$-ATPase and $H^+$-ATPase at 8-Å resolution, based on cryoelectron microscopy of two-dimensional crystals. These studies reveal the overall shape of these proteins and presence of 10 trans-membrane $\alpha$-helical rods most of which are tilted at an angle to the membrane (1, 2). These structural studies fit well with the trans-membrane topology of $\alpha$ subunits of P2-type pumps determined with a variety of biochemical techniques (3). Attempts are being made to infer the packing arrangement of the trans-membrane segments (1, 4). Biochemical and molecular studies are providing much information on functional sites for ATP and cations. The cation occlusion sites are located within trans-membrane segments as indicated by proteolysis experiments (5, 6) and site-directed mutagenesis (7, 8), and the latter approach suggests that carboxyl and other oxygen-containing side chains of residues within trans-membrane segments M4, M5, and M6, and probably M8, ligate the occluded cations (7–10). Thus, the trans-membrane helices are packed so as to create the cation occlusion "cage."

A biochemical approach for study of cation sites and the organization of trans-membrane segments utilizes renal $Na^+,K^+$-ATPase extensively digested with trypsin in the presence of $Rb^+$ ions (and absence of $Ca^{2+}$ ions) (5, 6). The digestion produces a preparation, referred to as 19-kDa membranes, that consists of well defined fragments of the $\alpha$ subunit, containing trans-membrane segments M7–M10 (apparent molecular mass ≈19 kDa) and the pairs M1/M2, M3/M4, and M5/M6 (apparent molecular mass 8–11.7 kDa), the $\beta$ subunit partially split into a 16-kDa N-terminal and ≈50-kDa C-terminal fragments, and intact $\gamma$ subunit. Cation occlusion and ouabain binding are fully maintained, but ATP binding is destroyed (5, 6, 11). These features indicate that cation occlusion sites are located within trans-membrane segments and communicate with ATP sites in the large cytoplasmic loop via the stalks of the membrane-embedded fragments. An advantage of 19-kDa membranes is their simplicity, and they have now been exploited in several ways. For example, strong protection by $Rb^+$ ions against further tryptic digestion of the 19-kDa and other fragments suggests that all fragments interact as a complex in which several trans-membrane segments cooperate to occlude the cations (12). Subsequently we have obtained direct evidence for the complex of fragments, containing occluded $Rb^+$ ions and bound ouabain, by solubilizing 19-kDa membranes with the non-ionic detergent $C_{12}E_{10}$ (13). Both the membrane-bound and detergent-solubilized complex of fragments have now also been used for covalent cross-linking, in order to define proximities of fragments and trans-membrane segments, leading to an approximate model of the helix packing arrangement (4, 14).

When 19-kDa membranes are incubated at 37 °C, their capacity to occlude $Rb^+$ ions or bind ouabain is rapidly lost (15, 16). The presence of occluded cations or ouabain protects strongly against this thermal inactivation of $Rb^+$ occlusion.

* This work was supported in part by a grant from the United States-Israel Binational Science Foundation. The costs of publication of this article were defrayed in part by the payment of page charges. This article must therefore be hereby marked "*advertisement*" in accordance with 18 U.S.C. Section 1734 solely to indicate this fact.

§ Supported by the State of Israel, Ministry of Absorption, the Center for Absorption of Scientist, and the Mauerberger Foundation, Cape Town, South Africa.

¶ To whom correspondence should be addressed. Tel.: 972 8 9342278; Fax: 972 8 344118; E-mail: steven.karlish@weizmann.ac.il.

Thermal inactivation has now been analyzed in detail and shown to be caused by disorganization of the interacting fragments (16). Following thermal disorganization the fragments become accessible to proteases in the medium and are digested to the limit membrane-embedded peptides (5, 12). Lutsenko *et al.* (17) reported the striking observation that incubation of 19-kDa membranes at 37 °C causes release into the medium of the fragment containing M5 and M6 ("the M5/M6 fragment"), associated with partial inactivation of $Rb^+$ occlusion. The presence of $Rb^+$ ions or ouabain protected against release of the fragment. The finding implies an important role for the M5/M6 fragment in occlusion of cations and also that it is stabilized by interactions with other fragments, such as the M7/M10 fragment as suggested by chemical labeling experiments (17, 18). More recently, using an antibody raised against the peptide $Leu^{815}$-$Gln^{828}$ within the M5/M6 fragment, we have found that only about 50% of the fragment is released and dissociation of the fragment follows inactivation of $Rb^+$ occlusion which is complete (16). The conclusion is that dissociation of the M5/M6 fragment is a consequence of thermal disorganization of the complex of fragments which is the direct cause of inactivation of $Rb^+$ occlusion. Both the indirect and now direct cross-linking evidence (14) demonstrate interactions between the M5/M6 and M7/M10 fragments in native 19-kDa membranes and their disruption upon thermal inactivation of occlusion. Thus, whereas the importance of the M5 and M6 trans-membrane segments in cation occlusion and transport is clear, the mechanism of the process is still unknown.

The $\beta$ subunit is an important component of both $Na^+,K^+$-ATPase and $H^+,K^+$-ATPase. The $\beta$ subunit stabilizes the $\alpha$ subunit and is required for functional expression of the pump at the plasma membrane (19, 20). The $\beta$ subunit interacts with the $\alpha$ subunit strongly in the extracellular loop L7/8 particularly in the sequence SYGQ (21, 22). Two points of interaction on the ectodomain of $\beta$ subunit have now been identified, before the first S–S bridge and between the second and third S–S bridges, respectively (23, 24). There is also evidence for $\alpha$-$\beta$ interactions mediated by the trans-membrane segment (25, 26) and cytoplasmic domains (27, 28) of the $\beta$ subunit. $\alpha$-$\beta$ interactions affect kinetic properties including interactions of $K^+$ and $Na^+$ ions with the pump (23, 27–32). Functional interactions occur particularly via the extracellular subunit interaction in L7/8, whereas functional cytoplasmic $\alpha$-$\beta$ interactions remain to be established. An additional use of 19-kDa membranes has been for chymotryptic digestion of the $\beta$ subunit. Incubation of 19-kDa membranes with $\alpha$-chymotrypsin at 37 °C in a $Rb^+$-containing medium leads to selective truncation of the N-terminal 16-kDa fragment of the $\beta$ subunit and eventually to inactivation of $Rb^+$ occlusion (27). Selective cleavage occurs in two steps, first truncation of the 16-kDa fragment (N terminus $Ala^5$) to a 15-kDa fragment (N terminus $Ile^{15}$) followed by further digestion to a 14-kDa fragment (N terminus $Leu^{24}$). After the second truncation the $Rb^+$ occlusion becomes thermally inactivated, and finally, all the fragments are digested to the limit membrane-embedded peptides. The experiments indicate that the cytoplasmic domain of the $\beta$ subunit affects access of $Rb^+$ ions to the occlusion sites, presumably via an interaction with the $\alpha$ subunit, although the nature of that interaction remains unknown.

In a quite different approach for studying cations sites, we have developed high affinity organic analogues of alkali metal cations, with the object of producing reactive derivatives for labeling and mapping the sites. This led us to synthesize and characterize aryl bis-guanidinium derivatives ($mXBG^{2+}$[1] and $pXBG^{2+}$) (33) and more recently tris-isothiouronium derivatives (Br-$TITU^{3+}$ and $Br_2$-$TITU^{3+}$) (34). $mXBG^{2+}$, $pXBG^{2+}$, Br-$TITU^{3+}$, and $Br_2$-$TITU^{3+}$ competitively inhibit $Na^+$ or $Rb^+$ occlusion, stabilize the $E_1$ conformation of the enzyme, and block $Na^+,K^+$-ATPase activity. Thus they are competitive $Na^+$-like antagonists. They compete with either $Na^+$ or $K^+$ ions for transport sites at the cytoplasmic surface (35). The intrinsic dissociation constant $K_D$ for $pXBG^{2+}$ or $mXBG^{2+}$ is 5–10 $\mu$M, whereas $K_D$ values of Br-$TITU^{3+}$ and $Br_2$-$TITU^{3+}$ are much lower, about 0.5 and 0.2 $\mu$M, respectively. A detailed functional analysis indicates that, unlike $Na^+$ and $K^+$ ions, the competitive $Na^+$-like antagonists are not occluded. The findings led to a model for cation occlusion with two steps, an initial recognition site which is common for both transported cations and their antagonists, followed by occlusion only of transported cations (15). Thus the antagonists block cation transport and $Na^+,K^+$-ATPase activity at the entry port for the cations. Despite the utility of these antagonists for dissecting stages of cation transport, suitable reactive derivatives have not yet been made, and thus the site of interaction with the protein has not been identified.

This paper brings together a number of novel observations based on the two biochemical approaches described above. The conclusion is that the cytoplasmic loop between M6 and M7 of the $\alpha$ subunit serves as the entrance port to cation occlusion sites and point of interaction of both transported cations and the competitive $Na^+$-like antagonists. Furthermore, the N-terminal domain of the $\beta$ subunit participates or is in close proximity with the entrance to the cation sites.

## EXPERIMENTAL PROCEDURES

$Na^+/K^+$-ATPase was prepared from fresh pig kidney red outer medulla by the rapid procedure described by Jørgensen (36). Protein, by the method of Lowry, and ATPase activity were determined as described by Jørgensen (36). Specific activity was in the range 13–20 units/mg of protein. Before use, the enzyme was dialyzed at 4 °C against 1000 volumes of a solution containing 25 mM histidine, pH 7.0, and 1 mM EDTA (Tris). Standard conditions for preparation of tryptic 19-kDa membranes were as described in Ref. 6. After digestion, membranes were washed, suspended, and stored in a standard medium containing 25 mM imidazole, pH 7.5, 1 mM EDTA, to which 2 mM RbCl was added.

*Cation Occlusion Assays*—The $Rb^+$ occlusion assays were performed as described (37). $Na^+$ occlusion in the presence of oligomycin 250 $\mu$g/ml was measured as described (5).

*Digestion with $\alpha$-Chymotrypsin (See Ref. 27)*—19-kDa membranes (1–2 mg/ml) were suspended in the standard medium containing 10 mM RbCl, with the pH adjusted to 8.0 with Tris base, and were incubated with $\alpha$-chymotrypsin (1:40 w/w) at 37 °C for 1 h. This produces the preparation known as chymotryptic intermediate (see text). Other conditions for chymotryptic digestion are given in legends to figures. After digestion, 0.2 mM TPCK, 1 mM PMSF, and 150 mM KCl were added sequentially, and the membranes were incubated at room temperature for 10 min upon each addition. The membranes were diluted 15-fold with a solution of the standard medium containing also 150 mM KCl, 1 mM PMSF, 0.2 mM TPCK, centrifuged at 250,000 × $g$ for 1 h, and the pellet was resuspended in standard medium and incubated again with TPCK and PMSF for 10 min at room temperature. The suspension was centrifuged again and then washed and suspended in standard medium. These procedures completely inactivate chymotrypsin and remove traces of chymotrypsin adsorbed to the membranes.

*Thermal Inactivation of 19-kDa Membranes (See Ref. 16)*—Membranes were centrifuged and suspended in a medium containing 25 mM imidazole, pH 7.5, 1 mM EDTA, 0.1 mM RbCl and were then washed again and suspended in a $Rb^+$-free medium. The final free $Rb^+$ concentration was estimated to be less than 1 $\mu$M. 19-kDa membranes were

[1] The abbreviations used are: $mXBG^{2+}$, *m*-xylylene bisguanidinium; $pXBG^{2+}$, *p*-xylylene bisguanidinium; TPCK, tosyl-L-phenylalanine chloromethyl ketone; PMSF, phenylmethylsulfonyl fluoride; Tricine, *N*-[2-hydroxy-1-bis(hydroxymethyl)ethyl]glycine; PAGE, polyacrylamide gel electrophoresis; MES, 2-[*N*-morpholino]ethanesulfonic acid; PVDF, polyvinylidene difluoride; Br-$TITU^{3+}$, 1-bromo-2,4,6-tris(methylisothiouronium)benzene; $Br_2$-$TITU^{3+}$, 1,3-dibromo-2,4,6-tris methylisothiouronium)benzene; RH421, *N*-(4-sulfobutyl)-4-[4-(*p*-dipentylaminophenyl)butadienyl]-pyridinium, inner salt.

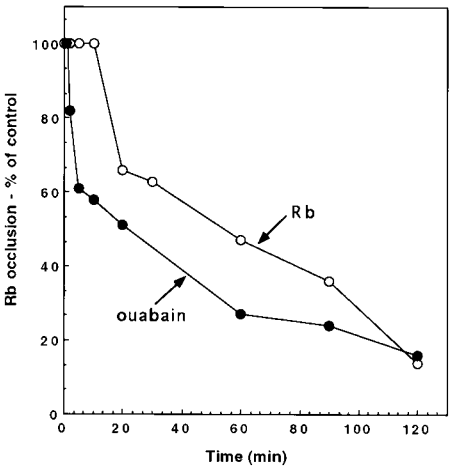


FIG. 1. **Inactivation of $Rb^+$ occlusion on 19-kDa membranes treated with chymotrypsin in the presence of ouabain or $Rb^+$ ions.** 19-kDa membranes (2 mg/ml) were pre-equilibrated at 20 °C for 40 min in the standard medium, pH 8.0, containing 10 mM RbCl (○) or 2 mM ouabain (●). Aliquots were transferred to 37 °C, and $\alpha$-chymotrypsin (1:5, w/w) was added. At indicated time, aliquots were withdrawn, and the reaction was stopped by addition of ice-cold reaction medium, containing 1.5 mM RbCl $^{86}Rb^+$, 100 mM Tris-HCl, pH 7.5, 1 mM PMSF, and 0.2 mM TPCK. Samples were incubated at room temperature for 20 min and then transferred to Dowex-50 columns for measurement of $Rb^+$ occlusion.

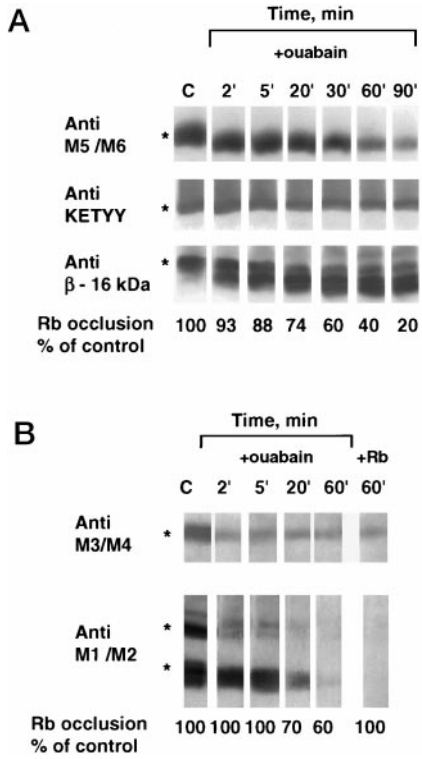


FIG. 2. **Chymotryptic digestion of 19-kDa membranes in the presence of ouabain, fragments detected with specific antibodies.** 19-kDa membranes (2 mg/ml) were pre-equilibrated at 20 °C for 40 min in the standard medium, pH 8.0, containing 2 mM ouabain. In the control TPCK inhibitor was added before chymotrypsin. *A* and *B,* represent two different experiments. The membranes were incubated at 37 °C with $\alpha$-chymotrypsin (1:10, w/w). At indicated times aliquots were withdrawn; the mixture of inhibitors was added, and samples were withdrawn for measurement of $Rb^+$ occlusion. The membranes were washed as described under "Experimental Procedures," and the samples were processed for SDS-PAGE. Equal amounts of delipidated protein (~10–20 $\mu$g) were applied per lane of a 10% Tricine gel. *Asterisks* designate the positions of relative fragments detected by the specific antibodies.

incubated at 0.5–2 mg/ml, in the conditions indicated in figure legends, in a thermostatically controlled water bath. At indicated times aliquots were placed on ice; reaction medium containing 1 mM RbCl plus $\approx 5 \cdot 10^6$ cpm $^{86}Rb$ was added, and $Rb^+$ occlusion was measured after a 60-min incubation at 0 °C or 5 min at 20 °C. Experimental points represent averages of duplicate samples. Variability between duplicates was less than 10%.

*Dissociation of the M5/M6 Fragment (See Ref. 16)*—19-kDa membranes (150 $\mu$g per sample) were diluted with 1 ml of a standard imidazole 25 mM, EDTA 1 mM buffer, pH 7.5, centrifuged at 250,000 × *g* for 1 h, and the pellet was resuspended in ice-cold medium containing either 10 mM Tris, 10 mM RbCl, or 1 mM $CaCl_2$. PMSF (100 mM) was added to all buffers to a final concentration of 1 mM. Samples were incubated at 37 °C. Aliquots were removed at a certain time and placed on ice. For electrophoretic analysis and immunoblots, the samples were transferred to ice, and the thermal inactivation was stopped by addition of ice-cold standard buffer containing 10 mM RbCl. The samples were centrifuged at 250,000 × *g* for 1 h. Pellets were resuspended in a standard medium of 25 mM imidazole, pH 7.5, 1 mM EDTA, and 2 mM RbCl. Prior to SDS-PAGE pellets were resuspended in standard medium, dissolved with 4% SDS, and protein was precipitated by addition of 4 volumes of ice-cold methanol and stored overnight at −20 °C. The delipidated protein was collected by centrifugation for 30 min at 10,000 rpm in a Sorvall centrifuge, dried in a stream of nitrogen, and dissolved in 10% SDS or the sample buffer. The supernatants were collected, lyophilized, and dissolved in a sample buffer. Equal amounts of delipidated membrane protein (~100 $\mu$g for stain and 10 $\mu$g for immunoblot) and equivalent amounts of supernatant and pellet were applied per lane of 10% gels.

*Gel Electrophoresis*—Tricine-SDS-PAGE was done essentially according to Ref. 38 using either 1.5-mm thick 10% gels (10% T, 3% C separating gel, 11.5 cm, plus 4% T stacking gel, 1.5 cm) or 1-mm thick 16.5% gels (16.5% T, 6% C separating gel, 20 cm; 10% T spacing gel, 2 cm; and 4% T stacking gel, 1.5 cm). Full details of the electrophoresis procedure, including precautions to be taken prior to sequencing of fragments, were given (6). Scanning of transparencies of photographs of gels were performed with a Molecular Dynamic 300A Computing Densitometer. For evaluating the effect of $Ca^{2+}$ on mobility of fragments, all solutions for preparing the gels and running and loading buffers were prepared to contain either 1 mM $Ca^{2+}$ or 0.1 mM EGTA (39).

*Immunoblots*—Immunoglobulins raised against the synthetic peptide ($Leu^{815}$-$Gln^{828}$) were supplied by Dr. J. V. Møller (Aarhus University). These serve for detection of the M5/M6 fragment. Anti-K1012-Y1016, referred to as "anti-KETYY" was supplied by Dr. J. Kyte (University of California San Diego, La Jolla) and is used to detect the M7/M10 fragment. Rabbit antisera, prepared as described in Ref. 40, were raised against fragments of 19-kDa membranes (5, 6) and include the following: 1) "anti-M1/M2," prepared from a 11.7-kDa fragment D68-R168, containing M1 and M2, and 2) "anti-$\beta$," prepared from a 16-kDa fragment $Ala^5$-$Arg^{142}$ of the $\beta$ subunit. For detection of the M3/M4 fragment anti-peptide antibodies were also raised against the synthetic peptides $Leu^{337}$-$Asn^{348}$ and $Ile^{263}$-$Pro^{276}$ coupled to keyhole limpet hemocyanin. Antibodies were diluted 1:100–1:400 in a solution of 1.5% (w/v) bovine serum albumin in TBS solution. Samples were delipidated, separated on 16.5% and 10% Tricine gels, and electroblotted onto PVDF paper using a Semi-Phor TE70 semi-dry transfer apparatus (Hoefer Scientific Instruments). Immunoblot analysis was described previously in detail (6).

*Fluorescence Measurements*—Fluorescence measurements were carried out in a Perkin-Elmer LS 50B fluorescence spectrophotometer as described (41). The thermostatically regulated cell holder was equipped with a magnetic stirrer. The excitation wavelength was set to 580 nm and the emission wavelength to 650 nm (slit width 15 and 20 nm, respectively). Sodium equilibrium titration experiments were performed in buffer containing 25 mM histidine, pH 7.2, 0.5 mM EDTA. 300 mM choline chloride, 200 nM RH421, and 9–10 $\mu$g/ml membrane fragments containing native or digested $Na^+$,$K^+$-ATPase were added to the cuvette and equilibrated until a stable fluorescence signal, $F_0$, was obtained. To allow a comparison between different titration experiments relative fluorescence changes, $\Delta F/F_0 = (F - F_0)/F_0$, were calculated (in %) with respect to the initial fluorescence intensity $F_0$ in the absence of $Na^+$ ions. All experiments were performed at 8 °C.

*Calculations*—Linear and nonlinear regression analyses were done using the program Enzfitter (Elsevier Bio-Soft). The predict protein server at the EMBL in Heidelberg was used to obtain a secondary structure prediction of the first 44 amino acids of the cytoplasmic portion of the $\beta$ subunit. The prediction was modeled on a Silicon

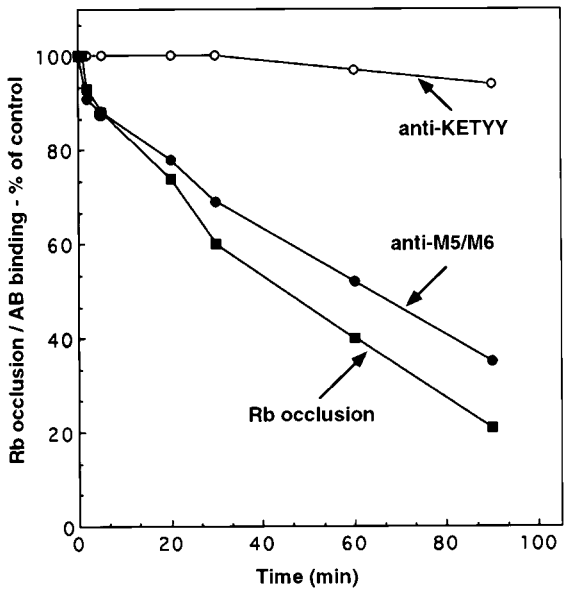


FIG. 3. **Chymotryptic digestion of 19-kDa membranes in the presence of ouabain, correlation of remaining $Rb^+$ occlusion with the M5/M6 fragment.** For details see under "Experimental Procedures" and Fig. 1. The amounts of M5/M6 and M7/M10 fragments remaining at each time were estimated by scanning the immunoblots.

Graphics computer using the program O (42) in order to obtain coordinates for a three-dimensional representation of the structure that was the drawn on a personal computer using the program RASMOL.

*Materials*—$^{86}$RbCl or $^{22}$Na was obtained from NEN Life Science Products. Dowex 50W-X8 (100 mesh) $H^+$-form (converted to Tris-form before use) was obtained either from Sigma or Fluka. TPCK, PMSF, MES, iodoacetamide, thioglycolate, and molecular weight markers (2.5–16.9-kDa) were from Sigma. Choline chloride (recrystallized from hot ethanol) was obtained from Fluka. α-Chymotrypsin was obtained from Merck. For SDS-polyacrylamide gel electrophoresis, all reagents were of electrophoresis grade from Bio-Rad. PVDF paper was from Millipore. RH421 was from Molecular Probes, Eugene, OR. Dye purity was checked by thin layer chromatography.

## RESULTS

*Selective Chymotryptic Cleavage of L6/7 Inactivates $Rb^+$ Occlusion*—As described in the Introduction, incubation of 19-kDa membranes with chymotrypsin in a medium containing $Rb^+$ ions, leads to inactivation of $Rb^+$ occlusion after a lag period, indicative of a two-step cleavage of the cytoplasmic domain of the β subunit (27). While screening different conditions of chymotryptic digestion we noticed that in a medium containing ouabain, inactivation of $Rb^+$ occlusion was quicker and showed no lag (Fig. 1).[2] Thus the pathways of cleavages in the ouabain medium might differ from that in the Rb medium. As a test of this possibility, cleavage of all the different fragments was examined in a medium containing ouabain, in parallel with measurement of $Rb^+$ occlusion (Fig. 2). Immunoblots were scanned, and the amount of each fragment was compared with the remaining $Rb^+$ occlusion capacity. The result was that a good correlation was found between the amount of remaining M5/M6 fragment and the $Rb^+$ occlusion (Fig. 3). Loss of antibody staining indicates that the M5/M6 fragment was cleaved within the epitope $Leu^{815}$-$Gln^{828}$, which straddles part of M6 and L6/7 (see Fig. 5), presumably at $Leu^{815}$, $Ala^{816}$, $Tyr^{817}$, or $Ala^{820}$ near the cytoplasmic surface. By contrast, the 19-kDa fragment was not cleaved (depicted also in Fig. 2*A*). The 16-kDa fragment of the β subunit was cleaved to the 15-kDa fragment (Fig. 2*A*), and the M1/M2 and M3/M4 fragments were also cleaved (Fig. 2*B*), but in these cases the cleavages clearly preceded loss of $Rb^+$ occlusion and cannot therefore be responsible for loss of occlusion. A previous observation that, in conditions in which the L6/7 is not cleaved, chymotrypsin truncates both the 16-kDa fragment and the M1/M2 fragments without inactivating $Rb^+$ occlusion supports the latter inference (see Ref. 27). Correlation of cleavage in L6/7 with inactivation of $Rb^+$ occlusion implies a close connection of L6/7 and the occlusion sites of the cations (see under "Discussion").

[2] In the presence of $Mg^{2+}$ ions ouabain is bound tightly and inhibits $Rb^+$ occlusion essentially irreversibly. In the absence of $Mg^{2+}$ ions, as in Fig. 1, binding of ouabain is of low affinity and is reversible upon incubation with $Rb^+$ ions (16). The latter feature permits measurement of $Rb^+$ occlusion after incubation of 19-kDa membranes with ouabain.

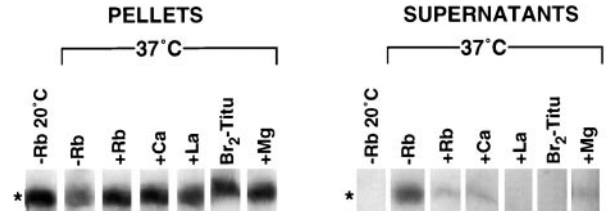


FIG. 4. **Protection by different cations against dissociation of the M5/M6 fragment from 19-kDa membranes.** Immunoblots using anti-$Leu^{815}$-$Gln^{828}$ depict the region between 6 and 8 kDa. For details of procedures and immunoblots using anti-$Leu^{815}$-$Gln^{828}$ see under "Experimental Procedures." *Asterisks* designate the position of the M5/M6 fragment.

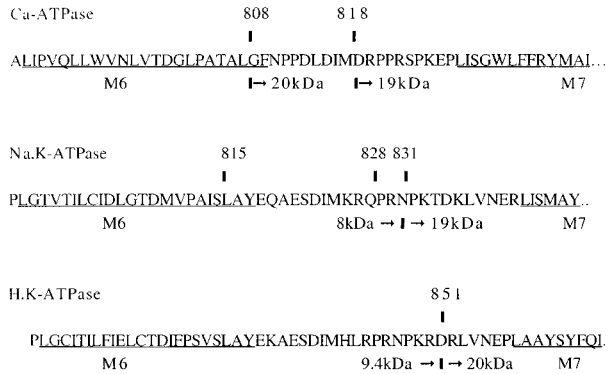


FIG. 5. **Sequence comparisons and proteolytic cleavage sites in L6/7 of α subunits of $Ca^{2+}$-, $Na^+$,$K^+$-, and $H^+$,$K^+$-ATPases.**

*Evidence for an Interaction of L6/7 with Divalent and Trivalent Cations*—Previously we used the specific anti-$Leu^{815}$-$Gln^{828}$ antibody and showed that dissociation of the M5/M6 fragment from 19-kDa membranes which occurs at 37 °C (17) follows inactivation of $Rb^+$ occlusion, and only about 50% of the fragment is released (16). In addition to $Rb^+$ or ouabain (17) $Ca^{2+}$ ions were found to prevent dissociation of the M5/M6 fragment (16). $Ca^{2+}$ ions compete with $Rb^+$ ions and are thought to be occluded in an abnormal state (12, 43, 44), but unlike $Rb^+$ ions or ouabain, $Ca^{2+}$ ions do not protect against thermal inactivation of $Rb^+$ occlusion in 19-kDa membranes (12, 16). In an extension of the previous observation, we have now looked at the effects of various divalent and trivalent cations on dissociation of the M5/M6 fragment. The cations $Mg^{2+}$ (11, 45), $La^{3+}$ (46) ions, $mXPG^{2+}$ and $pXBG^{2+}$ (33), and Br-$TITU^{3+}$ and $Br_2$-$TITU^{3+}$ (34) have in common the property that they compete with $Rb^+$ or $Na^+$ ions for occlusion sites and stabilize the $E_1$ conformation. Thus they are all $Na^+$-like competitive antagonists at the cytoplasmic surface. Unlike $Rb^+$ ions or ouabain, none of these $Na^+$-like competitive antagonists protect against thermal inactivation of $Rb^+$ occlusion (15, 16). Fig. 4 depicts the amount of M5/M6 fragment released into the medium and that remaining in the pellet after the 19-kDa membranes were incubated at 20 or at 37 °C in the indicated conditions. Significant dissociation of the M5/M6 fragment oc-

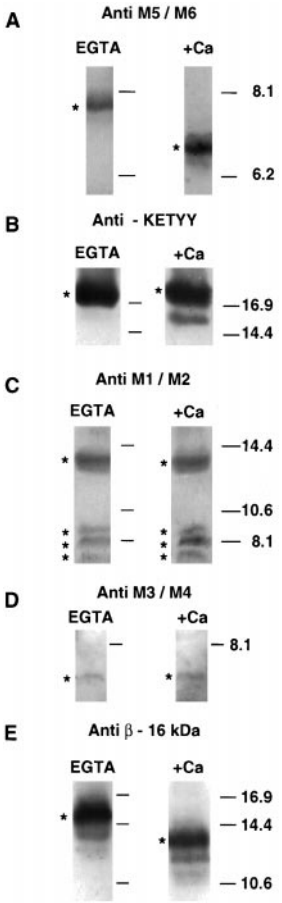


FIG. 6. **Effect of $Ca^{2+}$ ions on electrophoretic mobility of fragments of 19-kDa membranes.** SDS-PAGE was performed as described under "Experimental Procedures" with either 0.1 mM EGTA or 1 mM $Ca^{2+}$. *Asterisks* designate the positions of relative fragments detected by specific antibodies. *A,* anti-M5/M6; *B,* anti-KETYY; *C,* anti-M1/M2; *D,* anti-M3/M4; and *E,* anti-$\beta$-16 kDa. *Lines* depict the position of low molecular weight markers.

curred only at 37 °C in the Tris-HCl medium and to an extent of about 50% (16). Dissociation was largely prevented either in media containing $Rb^+$ ions or in media containing $Ca^{2+}$, $La^{3+}$, $Mg^{2+}$ ions and $Br_2$-$TITU^{3+}$.

A simple hypothesis to explain how divalent and trivalent cations prevent dissociation of the M5/M6 fragment is that these cations bind to the M5/M6 and to other fragments or perhaps phospholipid so anchoring the M5/M6 fragment to the membrane. $Ca^{2+}$-binding proteins or peptides (39, 47) can show changes in electrophoretic mobility upon binding of $Ca^{2+}$ ions. By using this feature it was shown recently that residues in the cytoplasmic loop L6/7 of sarcoplasmic reticulum $Ca^{2+}$-ATPase bind $Ca^{2+}$ ions (39). Protease K treatment produced, among others, two fragments cleaved within L6/7, with N termini $Gly^{818}$ and $Asp^{808}$ and molecular mass values of 19 and 20 kDa, respectively. The 20-kDa fragment but not the 19-kDa fragment ran faster on the gel in the presence of $Ca^{2+}$ ions. Accordingly, charged residues within the segment $^{808}$GFNPPDLDIM$^{817}$ were proposed to bind $Ca^{2+}$ ions. Fig. 5 depicts sequences around L6/7 for $Ca^{2+}$-, $Na^+$,$K^+$-, and $H^+$,$K^+$-ATPases as well as proteolytic cleavage sites in L6/7 (and for $Na^+$,$K^+$-ATPase, the position of $Leu^{815}$-$Gln^{828}$ used to prepare the antibody). The comparisons show that segments homologous to $^{808}$GFNPPDLDIM$^{817}$ of $Ca^{2+}$-ATPase, namely $^{816}$AYEQAESDIM$^{825}$ of $Na^+$,$K^+$-ATPase and $^{833}$AYEKAESDIM$^{842}$ of $H^+$,$K^+$-ATPase, are located in the M5/M6 fragments

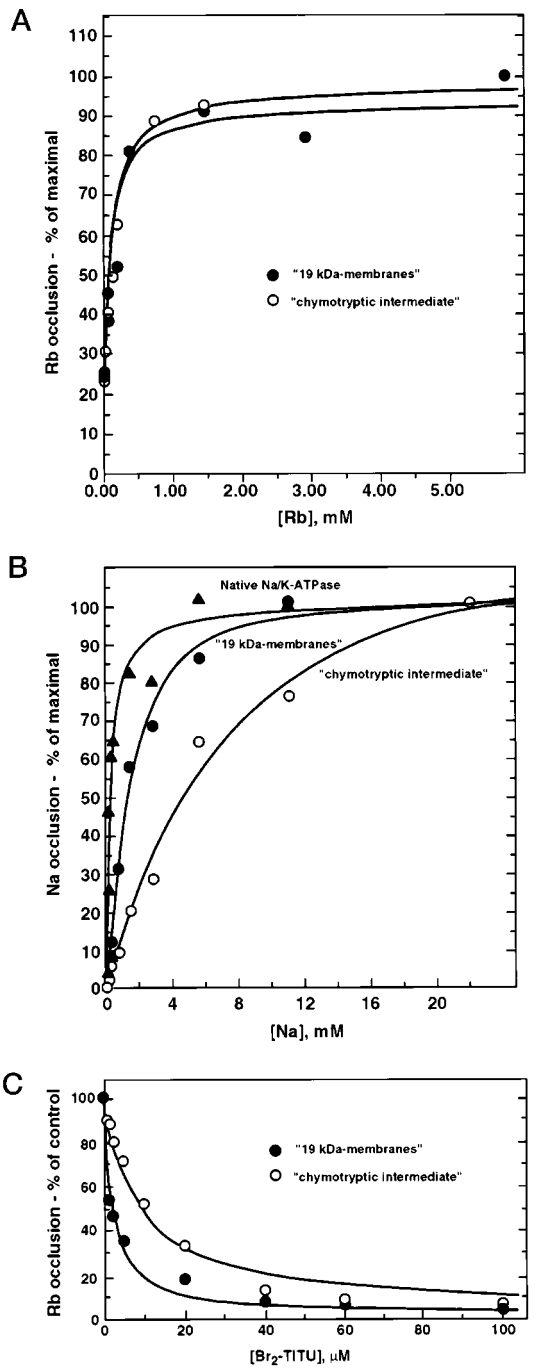


FIG. 7. **Comparison of $Rb^+$ occlusion (*A*), $Na^+$ occlusion (*B*), and $Br_2$-$TITU^{3+}$ binding (*C*) in native $Na^+$,$K^+$-ATPase (▲), 19-kDa membranes (●), and chymotryptic intermediate (○).** Native $Na^+$,$K^+$-ATPase, 19-kDa membranes, or chymotryptic intermediates (1 mg/ml) were incubated at 20 °C in 20–40 $\mu$l of the standard medium, pH 7.5, containing either 15–5000 $\mu$M RbCl $^{86}Rb^+$ (*A*) or 20 $\mu$M to 20 mM NaCl + $^{22}$Na plus oligomycin 250 $\mu$g/ml (*B*), or 50 $\mu$M $^{86}Rb^+$ plus 0.20–100 $\mu$M $Br_2$-$TITU^{3+}$ (*C*). Ionic strength was kept constant with choline chloride. The data were obtained from experiments employing the same 19-kDa membranes or "chymotryptic intermediate." The *continuous lines* were drawn according to Michaelis-Menten equation (*A*), best fit parameters to the Hill equation (*B*), and best fits to the expression $R = K_i/([Br_2\text{-}TITU^{3+}] + K_i)$ where $R$ is the ratio of $Rb^+$ occlusion with or without Br2-$TITU^{3+}$ present, and $K_i$ is the apparent inhibition constant (*C*).

of the tryptically digested $Na^+$,$K^+$- or $H^+$,$K^+$-ATPases (8 or 9.4 kDa, respectively) (6, 48).

Based on the comparisons in Fig. 5, the experiment of Fig. 6 looked at the possibility that the M5/M6 or other fragments in

TABLE I
*Kinetic parameters for cation binding to native Na,K-ATPase, 19-kDa membranes, and the chymotryptic intermediate*

| | $Rb^+$ occlusion $K_{0.5}$ | $Na^+$ occlusion, with oligomycin | | Br-TITU$^{3+}$ binding, $K_i$ | Electrogenic $Na^+$ binding | |
|---|---|---|---|---|---|---|
| | | $K_{0.5}$ | $n_H$ | | $K_{0.5}$ mM, $-Mg^{2+}$ | $K_{0.5}$ mM, + 10 mM $Mg^{2+}$ |
| | $\mu M$ | $mM$ | | $\mu M$ | | |
| Native $Na^+$, $K^+$-ATPase | 47 ± 3 (5) | 0.59 ± 0. | 0.9 ± 0.141 | 0.31 ± 0.06 (34) | 0.37 ± 0.01 | 3.7 ± 0.13 |
| 19-kDa membranes | 31.6 ± 3.9 | 1.11 ± 0.2 | 1.74 ± 0.28 | 2.59 ± 0.73 | 1.4 ± 0.04 | 3.9 ± 0.05 |
| Chymotryptic intermediate | 35.0 ± 8.7 | 7.95 ± 1.19 | 1.15 ± 0.1 | 9.5 ± 1.05 | 3.4 ± 0.39 | 5.0 ± 0.22 |

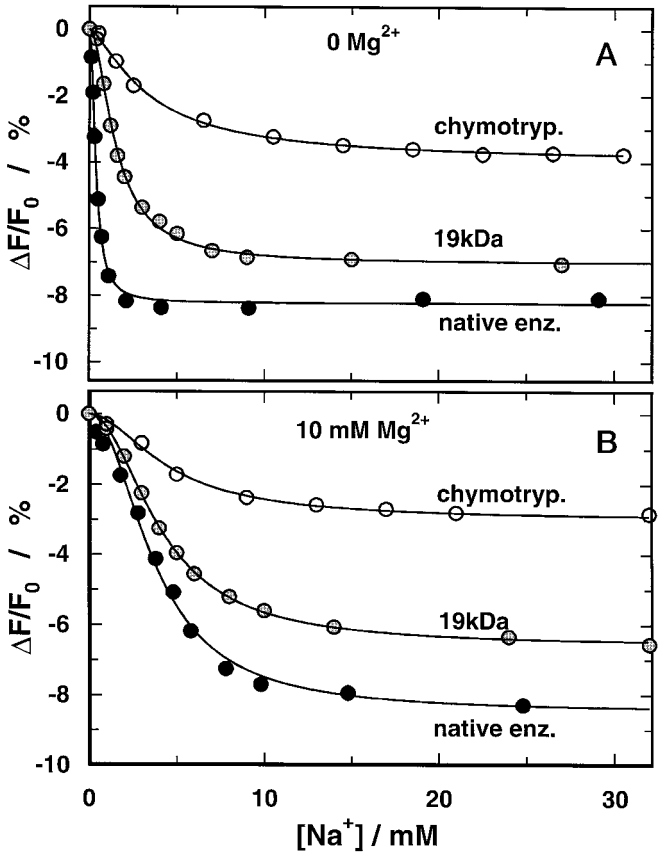


FIG. 8. **Comparison of electrogenic $Na^+$ binding in native $Na^+$,$K^+$-ATPase, 19-kDa membranes, and chymotryptic intermediate in the absence (*A*) and presence (*B*) of 10 mM $MgCl_2$.** Buffer composition was 300 mM choline chloride, 25 mM histidine, 0.5 mM EDTA, pH 7.2, at 8 °C. The data presented here are the average of three to five titration experiments. The RH421 fluorescence changes are attributed to electrogenic $Na^+$ binding to the cytoplasmic binding sites. Apparent binding constants from fits of the Hill function to the data are as indicated under "Results."

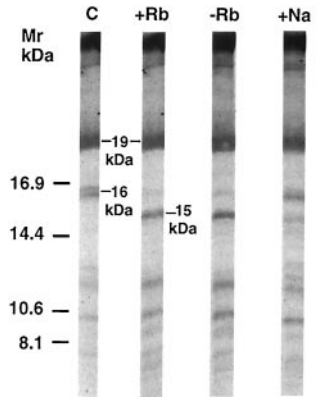


FIG. 9. **Chymotryptic cleavage of the β subunit at 20 °C in the absence or presence of $Na^+$ and $Rb^+$ ions.** Chymotryptic digestion (1:10, w/w) was done for 60 min at 20 °C as described under "Experimental Procedures." 19-kDa membranes (2 mg/ml) were pre-equilibrated at 20 °C for 40 min in the standard medium, pH 8.0, containing either 10 mM Tris-HCl, 10 mM RbCl, or 50 mM NaCl. Equal amounts of delipidated protein (~100 μg) were applied per lane of a 16.5% Tricine gel. *Left line*, low molecular weight markers, *second left line*, control 19-kDa membranes.

19-kDa membranes bind $Ca^{2+}$ ions and show changes in electrophoretic mobility in $Ca^{2+}$-loaded SDS gels. The result is that the M5/M6 fragment indeed migrated significantly faster in the $Ca^{2+}$-containing gel (Fig. 6*A*). By contrast, the M7/M10 fragment and M1/M2 and M3/M4 fragments, detected by specific antibodies (Fig. 6, *B–D*, respectively), did not change their mobility. Thus the M5/M6 fragment is the only one of the four fragments of the α subunit that changes its mobility in the presence of $Ca^{2+}$ ions, presumably because it binds $Ca^{2+}$ ions. An additional and unexpected result was that the 16-kDa N-terminal fragment of the β subunit also migrated faster in the $Ca^{2+}$-containing gel (Fig. 6*E*) (see under "Discussion").

*Selective Chymotryptic Cleavage of the Cytoplasmic Domain of the β Subunit*—Whereas incubation of 19-kDa membranes with chymotrypsin in a $Rb^+$-containing medium at 37 °C causes inactivation of $Rb^+$ occlusion following truncation of the 16-kDa fragment to 15 and then 14 kDa, incubation with chymotrypsin at 20 °C produces a stable 15-kDa fragment of the β subunit and intact $Rb^+$ occlusion (see Ref. 27 and also see Fig. 9). These stable membranes are referred to as the chymotryptic intermediate. In these membranes the maximal capacity for $Rb^+$ occlusion is unchanged (27). At 37 °C the apparent affinity for $Rb^+$ ions was reduced, and the dissociation rate of occluded $Rb^+$ ions was much increased compared with 19-kDa membranes (27). However, we have now found that when kinetics of $Rb^+$ occlusion are measured at 20 °C, the properties of $Rb^+$ occlusion are the same in 19-kDa membranes and the chymotryptic intermediate (Fig. 7 and Table I and see Ref. 27 for identical rates of dissociation of $^{86}Rb$ at 20 °C). By contrast, even at 20 °C, the chymotryptic intermediate displays a much lower apparent affinity for both $Na^+$ ions and $Br_2$-TITU$^{3+}$ (Fig. 7). The kinetic parameters for $Na^+$ occlusion as determined from the Hill function in the presence of oligomycin on native enzyme, 19-kDa membranes, and the chymotryptic intermediate are given in Table I. The difference between native enzyme and 19 kDa is similar to that reported previously (5), whereas the chymotryptic intermediate shows a much lower apparent affinity and Hill coefficient for $Na^+$ ions. Maximal capacities for $Na^+$ occlusion were the same in the 19-kDa membranes and chymotryptic intermediate. The $K_i$ values for $Br_2$-TITU$^{3+}$ were estimated from the apparent affinity for inhibition of $Rb^+$ occlusion at a low concentration of $Rb^+$ ions (Table I). The affinity for Br-TITU decreases sharply between native and 19-kDa membranes and decreases significantly again in the chymotryptic intermediate. Another way of looking at effects of the chymotryptic cleavage on $Na^+$ binding utilized the fluorescent dye RH421 which monitors the electrogenic $Na^+$ binding at an uncharged cytoplasmic binding site (41, 49). As seen in Fig. 8 the apparent affinity for electrogenic $Na^+$ binding to the chymotryptic intermediate was significantly reduced compared with the $Na^+$ affinity of 19-kDa membranes, itself lower than

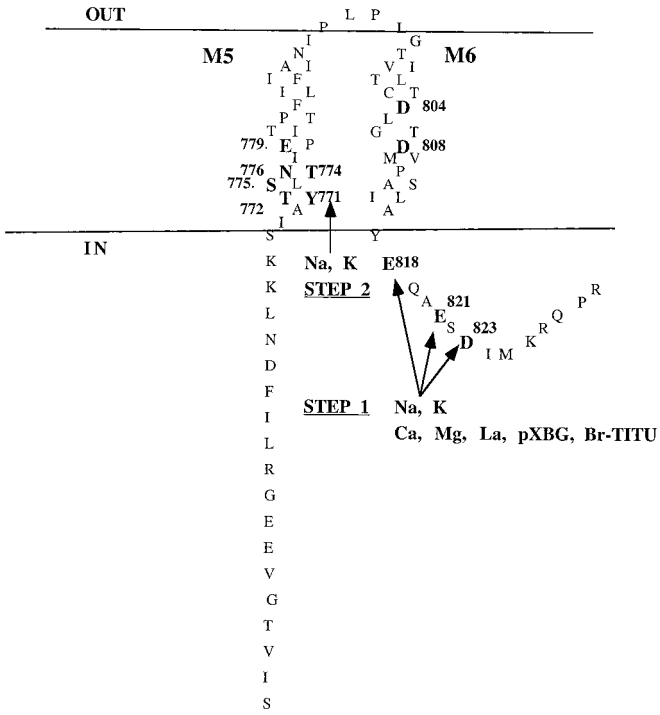


FIG. 10. **Model of M5/M6 hairpin and L6/7 of the $\alpha$ subunit indicating the two steps of cation occlusion.**

for binding to the native $Na^+$,$K^+$-ATPase (Fig. 8*A* and Table I). In the presence of 10 mM $Mg^{2+}$ ions (Fig. 8*B*), the apparent affinity for the electrogenic effect of $Na^+$ was significantly reduced in all preparations (Table I). The decrease in apparent $Na^+$ affinity was greatest in native enzyme, showing that the $Mg^{2+}$ ions compete more effectively in native enzyme compared with 19-kDa membranes and chymotryptic intermediate.

A necessary implication of the selective effect of the chymotryptic truncation of the $\beta$ subunit on $Na^+$ occlusion is that $Na^+$ ions should selectively affect the structural organization of the cytoplasmic domain of the $\beta$ subunit in these conditions. This hypothesis was tested in the experiment of Fig. 9 which examined the sensitivity of the 16-kDa fragment to chymotryptic digestion at 20 °C in media containing $Na^+$ or $Rb^+$ ions or lacking both $Rb^+$ and $Na^+$ ions. The result is clear cut. Truncation of the 16- to 15-kDa fragment occurred to an equal extent in media containing $Rb^+$ ions or lacking alkali metal cations, but it was largely prevented by the presence of $Na^+$ ions. We noted previously that the cytoplasmic truncation of the $\beta$ subunit is correlated with truncation of the M1/M2 fragment to slightly shorter forms with N terminus $Ala^{72}$ or $Thr^{74}$, instead of the normal $Asp^{68}$ (27). As seen in Fig. 9 $Na^+$ ions also protected the M1/M2 fragment against the chymotrypsin. In summary the experiment shows the following: 1) $Na^+$ ions selectively protected against the truncation of the $\beta$ subunit from the 16- to 15-kDa fragment and also the M1/M2 fragment, and 2) cleavage of the 16- to 15-kDa fragment of the $\beta$ subunit and also the truncation of the M1/M2 fragment does not require the presence of $Rb^+$ ions but occurs in a $Na^+$-free medium. Other experiments showed that the level of $Rb^+$ occlusion was not affected by incubation with chymotrypsin in any of these conditions (not shown).

## DISCUSSION

*Role of L6/7 in Cation Occlusion and Transport, Relation to M5 and M6*—How do the present findings add to what is already known from site-directed mutagenesis and biochemical evidence that residues in trans-membrane segments M4, M5, and M6 play a central role in occlusion of $Na^+$ and $K^+$ ions? Chymotryptic cleavage in L6/7 associated with inactivation of $Rb^+$ occlusion (Fig. 3) could indicate either that residues within L6/7 are directly involved in the cation occlusion and transport path or that the cleavage indirectly perturbs residues within M5 and M6 which ligate occluded cations. However, the other findings in Figs. 4–6 suggest most simply that residues in L6/7 participate directly in the transport pathway, not as ligating groups for occluded cations but rather as an entrance port to the occlusion sites within the trans-membrane segments.

Protection by $Ca^{2+}$, $Mg^{2+}$, $La^{3+}$, or $Br_2$-$TITU^{3+}$ against dissociation of the M5/M6 fragment (Fig. 4) implies that these cations bind to this fragment and to other fragments or phospholipid head groups and so anchor the M5/M6 fragment to the membrane. The finding of an exclusive change in electrophoretic mobility of the M5/M6 fragment in the presence of $Ca^{2+}$ ions (Fig. 6) provides a direct indication for binding of $Ca^{2+}$ ions, presumably in the L6/7 segment as predicted in Fig. 5. The segment may retain sufficient native structure in SDS to bind the $Ca^{2+}$ ions and alter the mobility of the M5/M6 fragment. Binding of divalent or trivalent cations must involve negative charge and therefore it is significant that the electrophoretic mobility of all other fragments of the $\alpha$ subunit is unaffected by $Ca^{2+}$ ions although they contain many negatively charged residues. $Ca^{2+}$, $Mg^{2+}$, $La^{3+}$, or $Br_2$-$TITU^{3+}$ all block occlusion and transport of $Na^+$ and $K^+$ ions at the cytoplasmic entrance to the sites without themselves becoming occluded (11, 12, 33–35, 46). Thus we assume that $Ca^{2+}$, $Mg^{2+}$, $La^{3+}$, or $Br_2$-$TITU^{3+}$ interact with the L6/7 loop that forms the C-terminal section of the M5/M6 fragment at the cytoplasmic surface. The segment in L6/7 is suggested to bind the cation antagonists. $^{816}$AYEQAESDIM$^{825}$ contains three negatively charged residues $Glu^{818}$, $Glu^{821}$, and $Asp^{823}$. Site-directed mutagenesis of these residues has not been reported for $Na^+$,$K^+$-ATPase, but mutations of the homologous residues of $H^+$,$K^+$-ATPase (E834Q, E837Q, and D839N) inactivate phosphorylation (50). Mutations of the aspartate residues in L6/7 of $Ca^{2+}$-ATPase (D813A/D818A and D813A/D815A/D818A) lower the affinity for $Ca^{2+}$ ions but allow phosphorylation at high $Ca^{2+}$ concentrations (51). Thus, these residues may interact with $Ca^{2+}$ ions but do not appear to be essential for $Ca^{2+}$ occlusion, as could be expected for residues located outside trans-membrane segments.

The notion that emerges is that charged residues in L6/7, located at the cytoplasmic surface, contribute to the initial recognition of transported cations which then move into the occlusion sites within the membrane. Fig. 10 illustrates this concept for $Na^+$,$K^+$-ATPase, similar to a proposal for $Ca^{2+}$ binding to the $Ca^{2+}$-ATPase (51), and presumably it applies also to $H^+$,$K^+$-ATPase or other P2-type pumps. In the first step $Na^+$,$K^+$ or the cation antagonists are bound to the charged residues in L6/7. In a second step $Na^+$ and $K^+$ ions, but not the antagonists, move into a moiety formed by M4, M5/M6,and M8 where they are occluded, perhaps, by a movement of L6/7 functioning as a lid. The residues in M5 and M6 numbered in bold type have been shown by site-directed mutagenesis to be important for interaction with alkali metal cations (8–10, 52, 53).

The present findings have two other implications for the role of trans-membrane segments M5 and M6 in cation occlusion and transport. First, M5 and M6 seem to be mobile and change conformation in the inner and outer conformations, but the nature of the structural changes is unknown (3). Dissociation of the M5/M6 hairpin from 19-kDa membranes implies that M5 and M6 are stabilized within the membrane by protein-protein interactions and gave rise to the proposal that active cation

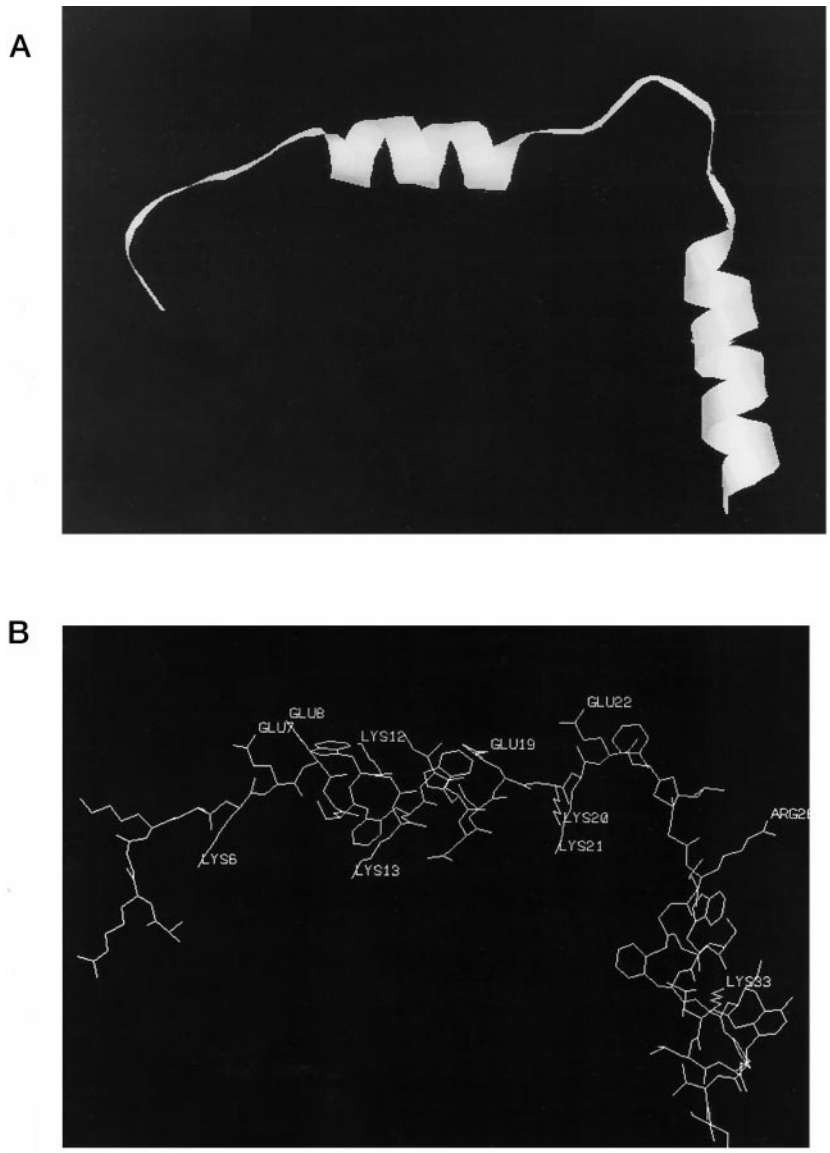


FIG. 11. **Predicted secondary structure of the cytoplasmic sector of the β subunit.** *A, ribbon*, and *B, wire* diagram.

transport normally involves a trans-membrane "piston-like" movement of M5 and M6 (17, 18, 55). Since, however, dissociation of the fragment occurs only from the thermally denatured 19-kDa membranes (16), and $Ca^{2+}$, $Mg^{2+}$, $La^{3+}$ and $Br_2$-$TITU^{3+}$ prevent its dissociation without protecting against thermal inactivation (Fig. 4), dissociation of the M5/M6 fragment cannot be used to argue for such movements in the native enzyme. More direct evidence against this possibility comes from direct cross-linking studies (14). Alternative possibilities for movement of M5 and M6 include twisting or change in the tilt of α-helices or changes in secondary structure in inner and outer facing conformations. Second, site-directed mutagenesis experiments indicate that both ouabain and $Rb^+$ ions bind to residues in the M5/M6 trans-membrane segments (among others) (10, 52–54). Cleavage of L6/7 by chymotrypsin only in the presence of ouabain (Fig. 2) implies that ouabain which binds from the outside induces a conformation that exposes L6/7 to chymotrypsin at the cytoplasmic surface. By contrast, occlusion of $Rb^+$ ions does not expose and may protect the L6/7 from chymotrypsin. This differential effect of ouabain over $Rb^+$ ions fits well with a proposal that ouabain inhibits the pump by stabilizing M5/M6 in a state which is unable to move (54), and of course supports the other evidence for mobility of the M5 and M6 segments in cation transport

*A Role for the Cytoplasmic Domain of the β Subunit*—The evidence presented here demonstrates that ion binding to the cytoplasmic sites is not only affected by the M5/M6 hairpin and the connecting L6/7 loop but, surprisingly, also by the cytoplasmic domain of the β subunit. Several findings are consistent with the assumption that the N terminus of the β subunit, particularly residues $Ala^5$-$Phe^{14}$, interacts with the cytoplasmic entrance to the alkali-metal cation sites.

The selective effect of cleavage at the $Phe^{14}$–$Ile^{15}$ bond on $Na^+$ occlusion or electrogenic $Na^+$ binding, without an effect on $Rb^+$ occlusion at 20 °C (Fig. 7), excludes a mere electrostatic effect and is explained most simply by assuming that the cytoplasmic domain of the β subunit interacts with cytoplasmic residues of the α subunit which determine selectivity for $Na^+$ over $K^+$ ions. Analysis of electrogenic $Na^+$ binding by RH421 fluorescence indicates that the two charged sites (that may also bind two $K^+$ ions) must be bound with two $Na^+$ ions prior to occupation of the neutral site (56). The large change in cooperativity for $Na^+$ occlusion in the chymotryptic intermediate indicates that not all cytoplasmic $Na^+$ sites are equally affected. A plausible explanation is that truncation of the β subunit affects the uncharged site so that $Na^+$ binding is affected but $K^+$ binding is not affected. This is supported by the observation that $Na^+$ ions selectively protect the bond at $Phe^{14}$-

Ile[15] of the β subunit, and also truncation of the M1/M2 fragment, against chymotryptic cleavage at 20 °C.

Which segments of the α subunit are candidates for cytoplasmic α-β interactions, bearing in mind that there may be more than one interaction?

One likely candidate is L6/7 itself or a point nearby. Since $Br_2$-TITU$^{3+}$ seems to bind in L6/7, the reduced $Br_2$-TITU$^{3+}$ affinity upon truncation of the β subunit suggests that $Br_2$-TITU$^{3+}$ binds directly to both L6/7 and Ala[5]-Phe[14] of the β subunit or that Ala[5]-Phe[14] interacts at or near L6/7. Binding of $Ca^{2+}$ ions to both M5/M6 fragments and the 16-kDa fragment of the β subunit (Fig. 6) is also consistent with a connection between the two fragments. The selective effect of the truncation of the β subunit on $Na^+$ binding and $Na^+$-selective protection against cleavage at that Phe[14]–Ile[15] bond suggests that this segment interacts with residues that affect cation selectivity, for example Thr[774] near the entrance to the tight hairpin M5/M6 (53), itself in close proximity to L6/7. The fact that truncation of the β subunit inactivates $Rb^+$ occlusion only at 37 °C and not at 20 °C (27) could imply that removal of the specific α-β interaction near M5 or L6/7 perturbs residues in M5 and M6 directly involved in occluding $Rb^+$ ions only at the higher temperature. A second candidate for interaction with Ala[5]-Phe[14] of the β subunit is the region near Asp[68] in the cytoplasmic segment of the α subunit before M1. Cleavage of the β subunit at the Phe[14]–Ile[15] bond is correlated with a small truncation of the M1/M2 fragment from Asp[68] to Ala[72] or Thr[74] (27), and both positions are protected against cleavage selectively by $Na^+$ ions. Based on properties of chimeric $Ca^{2+}$-ATPase and $Na^+$,$K^+$-ATPase molecules, the cytoplasmic segment between Gly[1] and Leu[65] has also been claimed to play a role in determining $Na^+$ selectivity (57).

Fig. 11 presents two views of the predicted secondary structure of the N-terminal 40 residues of the β subunit, including the cytoplasmic sequence Ala[1]-Lys[33] and a part of the transmembrane segment after Lys[33]. The prediction was done using the sequence from the pig β1 gene (see under "Experimental Procedures"), [1]ARGKAKEEGSWKKFIWNSEKKEFLGRTGG-SWF[33]KILLFTVI. The ribbon diagram visualizes unordered, helical, unordered, and then again a helical segment. The wire diagram shows that negatively charged residues within the first helix and loop face one way, and most of the positively charged residues face the other way. Charged residues could form salt bridges with partners in the α subunit and the glutamates could bind the cation antagonists as discussed above. A further indication for specific folding of the segment is that although there are many potential tryptic and chymotryptic cleavage sites, only a few splits are observed in the β subunit in 19-kDa membranes (5, 6, 27).

Truncation of the *Xenopus* β1 subunit before residue Lys[34] (Lys[33] in the pig sequence) raises the $K_{½}$ for both $K^+_{exc}$ and $Na^+_{cyt}$ ions for activating $Na^+$-$K^+$ exchange in *Xenopus* oocytes (25, 58). It has been reported recently that extensions of the truncated chain at the cytoplasmic side with a variety of unrelated sequences or replacement of sets of four residues with alanine produced pumps with wild-type values of $K_{½}$ for $K^+_{exc}$ and $Na^+_{cyt}$ (58). This has led to a proposal that the cytoplasmic truncation induces a trans-membrane conformational change that influences the known extracellular interactions of the β and α subunit in L7/8 (see Ref. 21). Although the findings in oocytes may be explained by this hypothesis, it does not fit well with our observations with 19-kDa membranes. The distinct and selective effect of chymotryptic cleavage at Phe[14]-Ile[15] on $Na^+$ occlusion and $Br_2$-TITU$^{3+}$ binding are difficult to explain without assuming cytoplasmic α-β interactions at the entrance to cation sites.

*Acknowledgment*—We are grateful for the support of E. Hofmann, University of Konstanz, for help in preparing the presentation of the three-dimensional structure of the cytoplasmic domain of the β subunit.

REFERENCES


1. Zhang, P., Toyashima, C., Yonekura, K., Green, N. M., and Stokes, D. L. (1998) *Nature* **392,** 835–839
2. Auer, M., Scarborough, G. A., and Kühlbrandt, W. (1998) *Nature* **392,** 840–843
3. Møller, J. V., Juul, B., and Le Maire, M. (1996) *Biochim. Biophys. Acta* **1286,** 1–51
4. Or, E., Goldshleger, R., and Karlish, S. J. D. (1999) *J. Biol. Chem.* **274,** 2802–2809
5. Karlish, S. J. D., Goldshleger, R., and Stein, W. D. (1990) *Proc. Natl. Acad. Sci. U. S. A.* **87,** 4566–4570
6. Capasso, J. M., Hoving, S., Tal, D. M., Goldshleger, R., and Karlish, S. J. D. (1992) *J. Biol. Chem.* **267,** 1150–1158
7. Rice, W. J., and Maclennan, D. H. (1996) *J. Biol. Chem.* **271,** 31412–31419
8. Jewell-Motz, E. A., and Lingrel, J. B. (1993) *Biochemistry* **32,** 13523–13530
9. Andersen, J. P., and Vilsen, B. (1995) *FEBS Lett.* **359,** 101–106
10. Nielsen, J. M., Pedersen, P. A., Karlish, S. J. D., and Jørgensen, P. L. (1998) *Biochemistry* **37,** 1961–1968
11. Schwappach, B., Stürmer, W., Apell, H.-J., and Karlish, S. J. D. (1994) *J. Biol. Chem.* **269,** 21620–21626
12. Shainskaya, A., and Karlish, S. J. D. (1994) *J. Biol. Chem.* **269,** 10780–10789
13. Or, E., Goldshleger, R., Tal, D. M., and Karlish, S. J. D. (1996) *Biochemistry* **35,** 6853–6864
14. Or, E., Goldshleger, R., and Karlish, S. J. D. (1998) *Biochemistry* **37,** 8197–8207
15. Or, E., David, P., Shainskaya, A., Tal, D. M., and Karlish, S. J. D. (1993) *J. Biol. Chem.* **268,** 16929–16937
16. Shainskaya, A., Nesaty, V., and Karlish, S. J. D. (1998) *J. Biol. Chem.* **273,** 7311–7319
17. Lutsenko, S., Anderko, R., and Kaplan, J. H. (1995) *Proc. Natl. Acad. Sci. U. S. A.* **92,** 7936–7940
18. Lutsenko, S., Daoud, S., and Kaplan J. H. (1997) *J. Biol. Chem.* **272,** 5249–5255
19. Geering, K. (1991) *FEBS Lett.* **285,** 189–193
20. Chow, D.-C., and Forte, J. D. (1995) *J. Exp. Biol.* **198,** 1–17
21. Fambrough, D. M., Lemas, M. V., Kamrick, M., Emerick, M., Renaud, K. J., Inman, E. M., Hwang, B., and Takeyasu, K. (1994) *Am. J. Physiol.* **266,** C579–C589
22. Colonna, T. E., Huynh, L., and Fambrough, D. M. (1997) *J. Biol. Chem.* **272,** 12366–12372
23. Bar Shimon, M., Goldshleger, R., and Karlish, S. J. D. (1998) *J. Biol. Chem.* **273,** 34190–34195
24. Melle-Milovanovic, D., Milovanovic, M., Nagpal, S., Sachs, G., and Shin, J. M. (1998) *J. Biol. Chem.* **273,** 11075–11081
25. Jaunin, P., Jaisser, F., Beggah, A. T., Takeyasu, K., Mangeat, P., Rossier, B. C., Horisberg, J.-D., and Geering, K. (1993) *J. Cell Biol.* **123,** 1751–1759
26. Eakle, K. A., Kabalin, M. A., Wang, S. G., and Farley, R. A. (1994) *J. Biol. Chem.* **269,** 6550–6557
27. Shainskaya, A., and Karlish, S. J. D. (1996) *J. Biol. Chem.* **271,** 10309–10316
28. Geering, K., Beggah, A., Good, P., Girardet, S., Roy, S., Schaer, D., and Jaunin, P. (1996) *J. Cell Biol.* **133,** 1193–1204
29. Lutsenko, S., and Kaplan, J. H. (1993) *Biochemistry* **32,** 6737–6743
30. Jaisser, F., Jaunin, P., Geering, K., Rossier, B. C., and Horisberger, J.-D. (1994) *J. Gen. Physiol.* **103,** 605–623
31. Eakle, K. A., Lyu, R.-M., and Farley, R. A. (1995) *J. Biol. Chem.* **270,** 13937–13947
32. Blanco, G., Koster, J., Sanchez, G., and Mercer, R. W. (1995) *Biochemistry* **34,** 319–325
33. David, P., Mayan, H., Cohen, H., Tal, D. M., and Karlish, S. J. D. (1992) *J. Biol. Chem.* **267,** 1141–1149
34. Hoving, S., Bar-Shimon, M., Tijmes, J. J., Goldshleger, R., Tal, D. M., and Karlish, S. (1995) *J. Biol. Chem.* **270,** 29788–29793
35. Or, E., Goldshleger, G., and Karlish, S. J. D. (1996) *J. Biol. Chem.* **271,** 2470–2477
36. Jørgensen, P. L. (1988) *Methods Enzymol.* **156,** 29–43
37. Shani, M., Goldshleger, R., and Karlish, S. J. D. (1987) *Biochim. Biophys. Acta* **904,** 13–21
38. Schägger, H., and von Jagow, G. (1987) *Anal. Biochem.* **166,** 368–379
39. Falson, P., Menguy, T., Corre, F., Bouneau, L., Gomez de Gracia, A., Soulié, S., Centeno, F., Møller, J. V., Champeil, P., and Le Maire, M. (1997) *J. Biol. Chem.* **272,** 17258–17262
40. Grossman, Z., Ram, D., Markovics, A., Tarrab-Hazdai, R., Lantner, F., Ziv, E., and Schechter, I. (1990) *Exp. Parasitol.* **70,** 62–71
41. Schneeberger, A., and Apell, H.-J. (1999) *J. Membr. Biol.* **168,** 221–228
42. Jones, T. A., Zou, J. Y., Cowan, S. W., and Kjeldgaard, M. (1991) *Acta Crystallogr. A* **47,** 110–119
43. Vassalo, P. M., and Post, R. L. (1986) *J. Biol. Chem.* **261,** 16957–16962
44. Forbush, B., III (1988) *J. Biol. Chem.* **263,** 7970–7978
45. Goldshleger, R., and Karlish, S. J. D. (1999) *J. Biol. Chem.* **274,** 16213–16221
46. David, P., and Karlish, S. J. D. (1991) *J. Biol. Chem.* **266,** 14896–14902
47. Klee, C. B., Crouch, T. H., and Krinks, M. H. (1979) *Proc. Natl. Acad. Sci. U. S. A.* **76,** 6270–6273
48. Shin, J. M., and Sachs, G. (1994) *J. Biol. Chem.* **269,** 8642–8646
49. Heyse, S., Wuddel, I., Apell, H.-J., and Stürmer, W. (1994) *J. Gen. Physiol.* **104,** 197–240

50. Swarts, H. G. P., Klaasen, C. H. W., De Boer, M., Fransen, J. A. M., and De Pont, J. J. H. H. M. (1996) *J. Biol. Chem.* **271,** 29764–29772
51. Menguy, T., Corre, F., Bouneau, L., Deschamps, S., Moller, J. V., Champeil, P., Le Maire, M., and Falson, P. (1998) *J. Biol. Chem.* **273,** 20134–20143
52. Kuntzweiler, T. A., Argüello, J. M., and Lingrel, J. B (1996) *J. Biol. Chem.* **271,** 29682–29687
53. Pedersen, P. A., Nielsen, J. M., Rasmussen, J. H., and Jorgensen, P. L. (1998) *Biochemistry* **37,** 17818–17827
54. Palasis, M., Kuntzweiler, T. A., Arguello, J. M., and Lingrel, J. B (1996) *J. Biol. Chem.* **271,** 14176–14182
55. Lutsenko, S., and Kaplan J. H. (1995) *Biochemistry* **34,** 15607–15613
56. Schultz, S., and Apell, H. J. (1995) *Eur. Biophys. J.* **23,** 413–421
57. Ishii, T., Lemas, V., and Takeyasu, K. (1994) *Proc. Natl. Acad. Sci. U. S. A.* **91,** 6103–6107
58. Hasler, U., Wang, X., Crambert, G., Beguin, P., Jaisser, P., Horisberger, J.-D., and Geering, K. (1998) *J. Biol. Chem.* **273,** 30826–30835